JOURNAL OF MATERIALS SCIENCE **36** (2001) 1901–1909

Cavitation instability in rubber with consideration of failure

W. J. CHANG, J. PAN*
Mechanical Engineering and Applied Mechanics, The University of Michigan, Ann Arbor, MI 48109, USA
E-mail: jwo@umich.edu

Cavitation instability in rubber is investigated by examining spherical void expansion in rubber particles under dead-load traction conditions. Spherical symmetry is assumed to simplify the governing equations in order to gain qualitative understanding of cavitation phenomenon. A simple strain failure criterion for rubber is proposed to demonstrate the effect of rubber failure on cavitation phenomenon. When the strain failure criterion is considered, the results show that, as in neo-Hookean materials, critical cavitation stresses exist for Mooney-Rivlin materials and for nonlinearly elastic materials characterized by a third-order strain energy function.

1. Introduction

Cavitation in rubber particles plays an important role in the toughening mechanism of rubber-modified plastics. It has been well known that addition of rubber particles to plastics can significantly increase the fracture toughness of the plastics. Yee and Pearson [1], Pearson and Yee [2, 3], and Yee *et al.* [4] observed that when rubber-modified epoxies were subject to loading, the rubber particles in the crack tip region were cavitated before noticeable plastic deformation of the matrix, and a massive shear yielding of the neighboring matrix followed the cavitation of rubber particles. Recently, Sue and Yee [5] investigated the influence of rubber particles and of pre-existing voids on the toughening of plastics and concluded that the major difference between pre-existing holes and cavitation in the rubber particles lies on the sudden buildup of the octahedral shear stress upon the cavitation of rubber particles in the crack tip region. Many research works have been conducted to understand the effects of rubber cavitation on toughening of plastics, for example, see Lazzeri and Bucknall [6, 7], Bucknall and Lazzeri [8], Huang and Kinloch [9], Steenbrink *et al.* [10], Steenbrink and Van der Giessen [11], Chen and Mai [12], Jansen *et al.* [13] and Jeong and Pan [14].

Jeong and Pan [14] investigated the deformation pattern near the tips of cracks in rubber-modified plastics. They assumed that the rubber particles were cavitated early in the deformation history and adopted a modified Gurson's yield criterion with consideration of the pressure sensitivity of the matrix to describe the plastic behavior of the rubber-modified plastics. Jeong and Pan [14] found that the computational results with the use of the void model to represent cavitated rubber particles in plastics agree well with the corresponding experimental results. As mentioned earlier, cavitation occurs early in rubber particles during the deformation history from experimental observations. Chang and Pan [15] examined the load-carrying capacity of rubber-modified plastics in order to understand the implications of the use of the void model to represent cavitated rubber particles in plastics. They found that rubber-modified plastics would have unrealistic large load-carrying capacity and voids grow quite slowly with increasing stress under spherically symmetrical loading conditions when higher-order strain energy functions are considered for rubber. This contradicts the experimental observations where cavities in rubber particles grows enormously near crack tips.

The theoretical model under spherically symmetrical conditions in Chang and Pan [15] is used to shed light on the material behavior near a crack tip under large hydrostatic tension conditions. The unrealistic large load-carrying capacity from using higher-order strain energy functions for rubber leads to an assumption of a failure criterion in Chang and Pan [15], where beyond certain strains the molecular chains in rubber break under biaxial stretching conditions. With this failure criterion, the load-carrying capacity of rubber-modified plastics is in agreement with the void model, and, consequently, the deformation pattern near crack tips can be reasonably explained by the fracture mechanics models (Jeong and Pan [14] and Al-Abduljabbar and Pan [16]). Computational models have been used to investigate the effects of rubber particles, rubber particles with finite size voids, and voids of equivalent particle sizes on the load carrying capacity and toughening of the plastic matrices (Huang and Kinloch [9], Steenbrink *et al.* [10], Steenbrink and Van der Giessen [11], Chen and Mai [12], Jeong and Pan [14], and Chang and Pan [15]).

* Author to whom all correspondence should be addressed.

However, in this paper, we concentrate on the cavitation instability and load carrying capacity of rubber itself.

There have been many research works on cavitation instability in rubber and metals. In general, cavitation instability occurs when the stress levels are sufficiently high such that the void expansion rate becomes infinitely large. Examples of material failure due to cavitation can be found in rubber (Gent and Lindley [17]) and in metals (Ashby *et al.* [18]), where voids grow enormously under the given conditions. Early work on cavitation instabilities is summarized in Hill [19]. The cavitation problem has been investigated in the context of nonlinear elasticity by Ball [20]. Ball studied a class of bifurcation problems in which a spherical void forms at the center of a sphere of nonlinearly elastic material under surface tractions or displacements.

An alternative interpretation of cavitation instability in terms of the growth of a pre-existing microvoid has been given by Horgan and Abeyaratne [21]. An excellent review of cavitation in nonlinearly elastic solids can be found in Horgan and Polignone [22]. For cavitation in elastic-plastic materials, Huang *et al.* [23] and Tvergaard *et al.* [24] examined cavitation instabilities in Mises materials under both spherically symmetric and axisymmetric conditions. Hou and Abeyaratne [25] examined the cavitation in elastic and elastic-plastic solids under non-symmetric loading and presented cavitation criteria in terms of the principal true stresses for neo-Hookean materials and elastic-plastic power-law materials. Chang and Pan [15] studied the load-carrying capacity of rubber-modified plastics with pre-existing voids in rubber particles with consideration of rubber failure at large strains. Williams and Schapery [26], Gent and Wang [27] and Lazzeri and Bucknall [6, 7] analyzed cavitation in rubber from the viewpoint of energy release rate.

Gent and Lindley [17] obtained the critical remote surface traction for a cavity in an infinitely thick spherical shell under radial traction conditions with the strain energy functions for neo-Hookean materials and modified Mooney-Rivlin materials. Their critical surface radial tractions are in the order of the elastic modulus and agree with those observed in the internal rupture of a thin rubber layer between two metal cylinders under tensile loads. As indicated by Gent and Lindley [17], the critical tractions are slightly lower with consideration of the failure of rubber at stretch ratios between 4 and 10 under biaxial stretching conditions. The theoretical framework of Ball [20] and Horgan and Abeyaratne [21] have provided insight into cavitation in nonlinearly elastic materials. However, the results of Hogan and Polignone [22] indicate that from the mathematical viewpoint, the critical radial tractions for the cavity become unbounded for Mooney-Rivlin materials or nonlinearly elastic materials characterized by higher-order strain energy functions.

One can imagine that for a given set of experimental stress-stretch ratio data under various loading conditions such as uniaxial tensile, biaxial tensile and simple shear loading conditions, a high-order strain energy function should have more flexibility to fit the experimental data under these various loading conditions. Neo-Hookean strain energy function may be used to fit some experimental data under various loading conditions, but cannot be the best choice to fit all data under various loading conditions, especially under large stretching conditions. Note that multiple coefficients in higher-order strain energy functions must be carefully selected as indicated in Kao and Razgunas [28].

For a given rubber, higher-order strain energy functions are supposed to be more accurate in characterizing stress-stretch ratio relations under more general multiaxial loading conditions. According to Hogan and Polignone [22], cavitation instability disappears when higher-order strain energy functions are used. For a given rubber, cavitation instability should not depend upon the selection of strain energy functions. Cavitation instability either does or does not exist. However, according to Hogan and Polignone [22], cavitation instability exists if a lower-order strain energy function is used whereas cavitation instability does not exist when a supposedly more accurate higher-order strain energy function is used. From this viewpoint, the mathematical framework to treat cavitation instability must be re-examined or re-interpreted to reflect the physical reality. Therefore, a strain failure criterion at large strains due to breaking of molecular chains is adopted in this paper to investigate cavitation instability in rubber when higher-order strain energy functions are used.

2. Constitutive modeling of rubber

Let us consider that a material point with the initial Cartesian coordinates X_i is displaced to a new position with the Cartesian coordinates x_i in an isotropic elastic solid. The deformation gradient tensor is defined as

$$F_{ij} = \frac{\partial x_i}{\partial X_j}, \tag{1}$$

and the left Cauchy-Green strain tensor is defined as

$$B_{ij} = F_{ik}F_{jk}. \tag{2}$$

The invariants of the tensor B_{ij} are

$$I_1 = B_{ii} \tag{3}$$

$$I_2 = \frac{1}{2}(B_{ii}B_{jj} - B_{ij}B_{ij}) \tag{4}$$

$$I_3 = \frac{1}{6}e_{ijk}e_{pqr}B_{ip}B_{jq}B_{kr} \tag{5}$$

where e_{ijk} is the permutation symbol.

It is generally accepted that under static loading conditions, rubbers are considered as isotropic hyperelastic incompressible materials. The strain energy function per unit undeformed volume for isotropic hyperelastic materials is generally expressed as a function of the three invariants, I_1, I_2 and I_3. The third invariant I_3 is identically equal to 1 because of the material incompressibility. Therefore, the strain energy function per unit undeformed volume for isotropic hyperelastic incompressible materials can be expressed in terms of I_1 and I_2 as

$$W = W(I_1, I_2). \tag{6}$$

Various forms of strain energy functions for Equation 6 have been suggested for incompressible materials.

We adopt a third-order strain energy function investigated by James, Green and Simpson [29] and James and Green [30]:

$$W = C_{10}(I_1 - 3) + C_{01}(I_2 - 3) + C_{11}(I_1 - 3)(I_2 - 3) + C_{20}(I_1 - 3)^2 + C_{30}(I_1 - 3)^3. \tag{7}$$

Note that Equation 7 reduces to the strain energy function for Mooney-Rivlin materials when $C_{11} = C_{20} = C_{30} = 0$ and reduces to that for neo-Hookean materials when $C_{01} = C_{11} = C_{20} = C_{30} = 0$. The components of the Cauchy stress, σ_{ij}, can be derived from W as [31]

$$\sigma_{ij} = -p\delta_{ij} + 2\frac{\partial W}{\partial I_1}B_{ij} - 2\frac{\partial W}{\partial I_2}(B^{-1})_{ij}, \tag{8}$$

where p is the hydrostatic pressure.

The material constants C_{ij} in Equation 7 are determined by fitting to the test data. Here, we consider a rubber with the material constants [32, 33]

$$C_{10} = 1.008 \times 10^{-1}\,\text{MPa} \tag{9}$$

$$C_{01} = 1.612 \times 10^{-1}\,\text{MPa} \tag{10}$$

$$C_{11} = 1.338 \times 10^{-3}\,\text{MPa} \tag{11}$$

$$C_{20} = 6.206 \times 10^{-4}\,\text{MPa} \tag{12}$$

$$C_{30} = 6.206 \times 10^{-9}\,\text{MPa}. \tag{13}$$

We also consider a Mooney-Rivlin material with the constants [34]

$$C_{10} = 0.550\,\text{MPa} \tag{14}$$

$$C_{01} = 0.138\,\text{MPa} \tag{15}$$

$$C_{11} = C_{20} = C_{30} = 0. \tag{16}$$

In addition, we consider a neo-Hookean material with the constants

$$C_{10} = 0.5\,\text{MPa} \tag{17}$$

$$C_{01} = C_{11} = C_{20} = C_{30} = 0. \tag{18}$$

For the neo-Hookean material, the only nonzero constant C_{10} is related to the shear modulus of rubber, G, as $C_{10} = G/2$. The values of G for rubbers generally lie between 0.2 and 1.0 MPa.

Note that the material constants C_{ij} are determined by fitting to the experimental data. When the deformation is larger than the deformation range of the experiment, unrealistic stress values at large strains can be predicted from these material constants. These constants may differ for the same material by fitting to the experimental data for different deformation ranges and loading conditions. However, a higher-order strain energy function should generally give a more accurate description of the material behavior at large strains under multiaxial loading conditions. The selection of the three representative rubbers with these material constants is to investigate the cavitation phenomena in these rubbers with and without consideration of rubber failure at large strains. In the following, we denote the material with the material constants in Equations 9 to 13 as the JGS material. We denote the Mooney-Rivlin material with the material constants in Equations 14 to 16 as the MR material. We denote the neo-Hookean material with the material constants in Equations 17 and 18 as the NH material.

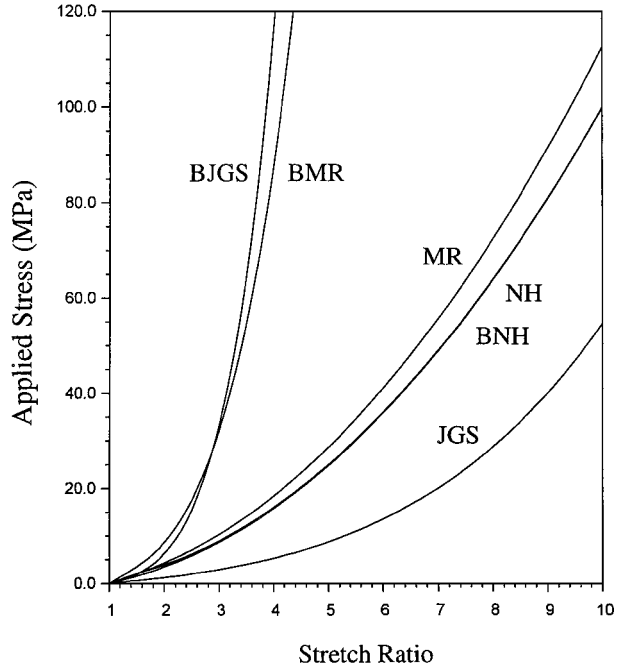

Figure 1 The stresses as functions of the stretch ratio for three nonlinearly elastic materials. Curves NH, MR, and JGS represent the NH, MR, and JGS materials under uniaxial tensile loading conditions, respectively. Curves BNH, BMR, and BJGS represent the NH, MR, JGS materials under equal biaxial tensile loading conditions, respectively.

In Fig. 1, the applied stresses as functions of the stretch ratio under uniaxial tensile loading and equal biaxial tensile loading for the JGS, MR, and NH materials are plotted. In the figure, the curves for the JGS, MR, and NH materials under uniaxial tensile loading are denoted by JGS, MR, and NH, respectively. The curves for the JGS, MR, and NH materials under equal biaxial tensile loading are denoted by BJGS, BMR, and BNH, respectively. Since the material elements on the void surface are subject to equal biaxial loading conditions (due to spherical symmetry), curves BJGS, BMR, and BNH in Fig. 1 represent the constitutive relations for these material elements and therefore have important implications on the modeling of void expansion in rubber particles. It should be noted that the neo-Hookean material (the NH material) has almost the same response at large stretch ratios under both uniaxial and biaxial tensile loading conditions, as shown by curves NH and BNH. The JGS and MR materials are very stiff under equal biaxial loading conditions. For example, curves BMR and BJGS in Fig. 1 show that the stresses at the stretch ratio $\lambda = 4$ are about 80 MPa and 120 MPa, which are larger than the yield stresses of the

typical plastic matrices in which the rubber particles are embedded for toughening. The stresses increase very sharply when the stretch ratio λ becomes larger than 4.

3. Governing equations

We now examine void expansion in rubber particles under spherically symmetric loading conditions. Fig. 2a depicts the undeformed configuration of a spherical rubber particle with a void. The rubber particle has the initial external radius r_0 and the initial void radius r_b. Fig. 2b schematically shows the deformed configuration of the rubber particle. In Fig. 2b, the external radius becomes R_0 and the void radius becomes R_b after a dead-load radial traction p_0 is applied at the outer boundary. The dead-load traction p_0 is related to the radial stress σ_R at $R = R_0$ based on the deformed configuration as

$$\sigma_R(R = R_0) = p_0 \left(\frac{r_0}{R_0}\right)^2, \tag{19}$$

as shown in Fig. 2b.

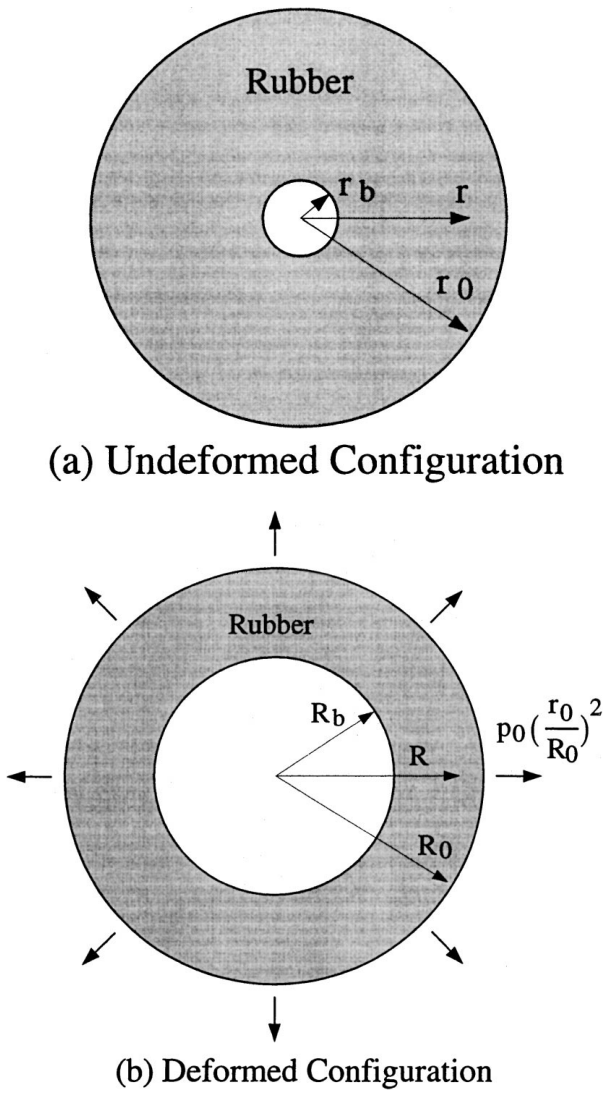

Figure 2 A void in a spherical rubber particle under radial dead-load traction p_0. (a) undeformed configuration, (b) deformed configuration.

We consider a spherical coordinate system with the three coordinates R, θ, and ϕ. The origin of the spherical coordinate system is located at the center of the void. Due to symmetry, the stretch ratio in the hoop direction, λ, can be simply represented as

$$\lambda = \frac{R}{r}, \tag{20}$$

where r and R represents the radial coordinate of a material point before and after deformation, respectively. Due to symmetry, the off-diagonal components of $\mathbf{B}$ are zero. The diagonal components of $\mathbf{B}$ are denoted as B_R, B_θ, and B_ϕ. From Equations 1 and 2, we have

$$B_\theta = B_\phi = \lambda^2. \tag{21}$$

The incompressibility gives

$$I_3 = B_R B_\theta B_\phi = 1. \tag{22}$$

Then, B_R can be found, by using (21) and (22), as

$$B_R = \lambda^{-4}. \tag{23}$$

Substituting Equations 21 and 23 into Equation 8 gives the relations between the stresses and the stretch ratio λ as

$$\begin{aligned}\sigma_R = &-p - 4C_{11}\lambda^6 + (-2C_{01} + 6C_{11})\lambda^4 + 24C_{30} \\ &+ (-72C_{30} + 8C_{20})\lambda^{-2} + (-6C_{11} + 54C_{30} \\ &+ 2C_{10} - 12C_{20})\lambda^{-4} + (4C_{11} + 24C_{30})\lambda^{-6} \\ &+ (4C_{20} - 36C_{30})\lambda^{-8} + 6C_{30}\lambda^{-12}\end{aligned} \tag{24}$$

$$\begin{aligned}\sigma_\theta = &-p + (2C_{11} + 24C_{30})\lambda^6 + (-72C_{30} + 8C_{20})\lambda^4 \\ &+ (-6C_{11} + 54C_{30} + 2C_{10} - 12C_{20})\lambda^2 + 24C_{30} \\ &+ (4C_{20} - 36C_{30} - 2C_{01} + 6C_{11})\lambda^{-2} \\ &+ (6C_{30} - 2C_{11})\lambda^{-6}\end{aligned} \tag{25}$$

$$\sigma_\phi = \sigma_\theta. \tag{26}$$

Here p will be determined by the equilibrium equation and the boundary conditions, and is a function of R. The off-diagonal stress components are equal to 0.

We now begin to solve for the stress distribution within the rubber particle. The equilibrium equation is

$$\frac{d\sigma_R}{dR} + \frac{2}{R}(\sigma_R - \sigma_\theta) = 0. \tag{27}$$

The boundary conditions require

$$\sigma_R = 0 \quad \text{at} \quad R = R_b. \tag{28}$$

Substituting Equations 24 and 25 into 27 gives

$$\frac{d\sigma_R}{dR} = \frac{2}{R}\{(6C_{11} + 24C_{30})\lambda^6 + (-72C_{30} + 8C_{20} + 2C_{01} - 6C_{11})\lambda^4 + (-6C_{11} + 54C_{30} + 2C_{10} - 12C_{20})\lambda^2 + (-4C_{20} + 36C_{30} - 2C_{01} + 6C_{11})\lambda^{-2} + (6C_{11} - 54C_{30} - 2C_{10} + 12C_{20})\lambda^{-4} + (-18C_{30} - 6C_{11})\lambda^{-6} + (-4C_{20} + 36C_{30})\lambda^{-8} - 6C_{30}\lambda^{-12}\} \quad (29)$$

The volume conservation due to incompressibility gives

$$R^3 - R_b^3 = r^3 - r_b^3. \quad (30)$$

Therefore, the stretch ratio λ in Equation 29 can be expressed as

$$\lambda = \frac{R}{r} = \frac{R}{\left(R^3 - R_b^3 + r_b^3\right)^{1/3}}. \quad (31)$$

Substituting $R = R_0$ into Equation 30 gives the expansion ratio of the outer radius of the rubber particle as

$$\frac{R_0}{r_0} = \left[1 - \left(\frac{r_b}{r_0}\right)^3 + \left(\frac{R_b}{r_0}\right)^3\right]^{\frac{1}{3}}. \quad (32)$$

Note that all the length scales are normalized by r_0 here. Also note that in Equation 32, the initial radius of the void r_b/r_0 is given as an input. For a given final void radius R_b/r_0, the governing equation (Equation 29) can be integrated from the deformed inner radius $R = R_b$ with the initial value of $\sigma_R = 0$ to the deformed outer radius R_0 which can be determined by Equation 32. At each R, p can then be determined from Equation 24. Once p is determined, σ_θ can be determined from Equation 25. The dead-load traction p_0 at $R = R_0$ can be obtained from Equation 19.

For a neo-Hookean material with the strain energy function

$$W = \frac{G}{2}(I_1 - 3), \quad (33)$$

the critical dead-load traction can be obtained (Gent and Lindley [17] and Ball [20]) as

$$p_{cr} = \frac{5G}{2}. \quad (34)$$

Also, Horgan and Polignone [22] obtained the relation between the applied traction and the current void radius by a Taylor expansion as

$$p_0 = p_{cr} + k\left(\frac{R_b}{r_0}\right)^3 + o\left(R_b^3\right), \quad (35)$$

where

$$k = \frac{2}{3}(p_{cr} - 2G). \quad (36)$$

From Equation 34 and $G = 2C_{10}$, we obtain $p_{cr} = 2.5$ MPa and $k = 1/3$ MPa for the NH material with the material constants in Equation 17.

It should be noted that the bifurcation model of cavitation can be successfully used to predict the critical traction for the internal rupture of the rubber observed by Gent and Lindley [17] when the rubber is modeled as a neo-Hookean material. The criterion for materials with strain energy functions to have a finite critical traction is given in Chou-Wang and Horgan [35], Polignone and Horgan [36], and Horgan and Polignone [22]. For example, when the strain energy function of the rubber is characterized by that of the Mooney-Rivlin materials or other higher-order strain energy functions [22], the critical traction becomes unbounded. However, the Mooney-Rivlin and other higher-order strain energy functions are considered to give more accurate description of the constitutive behavior of rubber at large strains. Therefore, it seems that a modification to the bifurcation approach is needed to reflect the fact that rubber cannot be extended to infinite stretch ratio.

4. Results

Because a rubber material element cannot be extended to infinite stretch ratio, a failure mechanism at large strains is considered. Note that the material elements on the void surface of the rubber particle are under plane stress, equal biaxial loading conditions. For investigation of the effects of a failure mechanism on cavitation, we adopt a simple failure criterion such that rupture occurs when the stretch ratio λ reaches a critical value under plane-stress, equal biaxial stretching conditions. Note that the failure stretch ratios are different for different rubbers. The failure stretch ratio depends upon the degree of cross-linking, stretch rate, and temperature. The values of the stretch ratio at failure in equibiaxial tension for vulcanised natural rubber are between 3.5 and 4.0 [6].

Here we just take $\lambda = 4$ as the failure stretch ratio for the three rubbers to explore the implications of a failure criterion on cavitation phenomenon. Therefore, when the stretch ratio λ of the material elements on the void surface of the rubber particle reaches the critical value of 4, the rubber material elements fail. In the pre-existing void model of cavitation, no limit is assumed on the maximum strain that the material can experience. Therefore, for an initially infinitesimal void growing to a finite size, the stretch ratios of the material elements on the void surface become infinite. Now, with consideration of a simple strain failure criterion, we examine the cavitation phenomena in the three rubbers characterized by different strain energy functions. The results for the neo-Hookean material, the Mooney-Rivlin material and the JGS material are shown in Figs 3–5, respectively.

For the neo-Hookean material with the material constants in Equations 17 and 18, the dead-load tractions (p_0) as functions of the normalized current void size (R_b/r_0) are shown as dash curves in Fig. 3 for various normalized initial void sizes (r_b/r_0). Curve A represents Equation 35 which is an approximate relation for

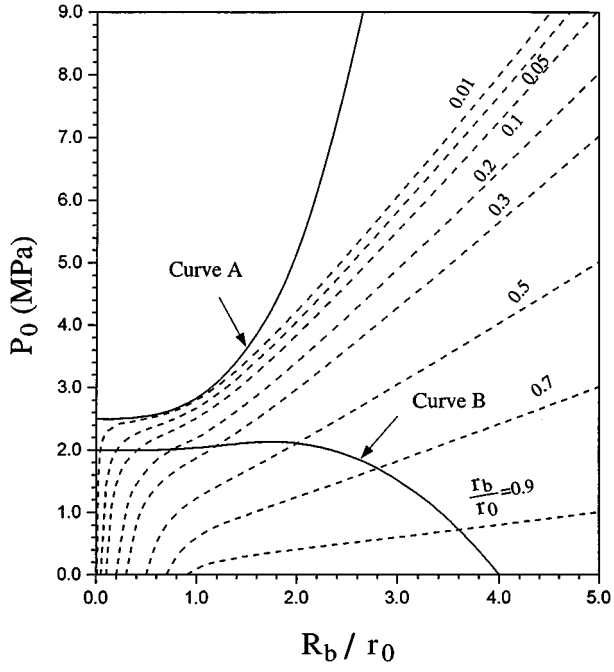

Figure 3 The relation between the applied traction p_0 and the current void size R_b/r_0 for a neo-Hookean material. The dashed curves represent the expansion ratios of the void with different initial sizes under dead-load traction conditions. Curve A represents an approximate relation for an initially infinitesimal void with no consideration of rubber failure. Curve B represents the critical tractions for various initial void sizes with consideration of rubber failure at $\lambda = 4$.

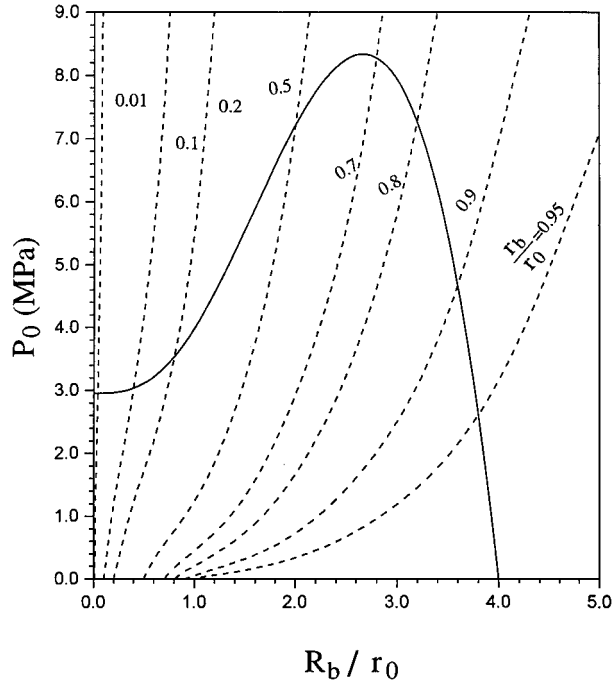

Figure 5 The relation between the applied traction p_0 and the current void size R_b/r_0 for a JGS material characterized by a third-order strain energy function. The dashed curves represent the expansion ratios of the void with different initial sizes under dead-load traction conditions. The solid curve represents the critical tractions for various initial void sizes with consideration of rubber failure at $\lambda = 4$.

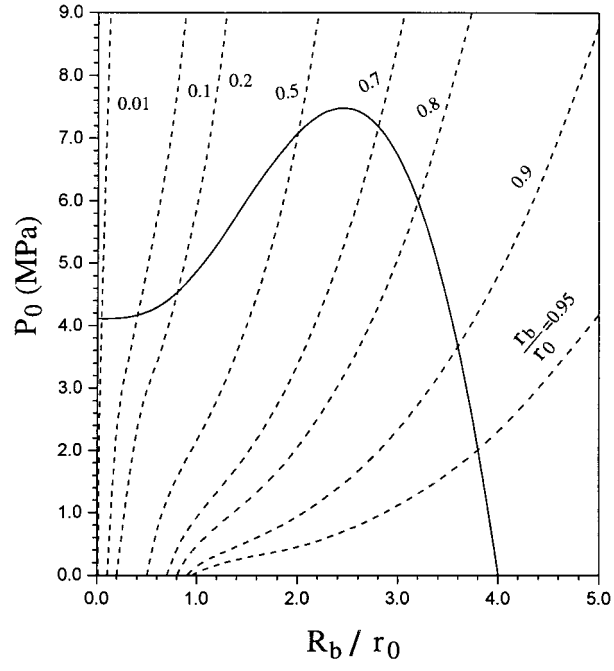

Figure 4 The relation between the applied traction p_0 and the current void size R_b/r_0 for a Mooney-Rivlin material. The dashed curves represent the expansion ratios of the void with different initial sizes under dead-load traction conditions. The solid curve represents the critical tractions for various initial void sizes with consideration of rubber failure at $\lambda = 4$.

an initially infinitesimal void. As shown in Fig. 3, when the normalized initial void size r_b/r_0 approaches to 0, the dashed curves approach to curve A. When the strain failure criterion at $\lambda = 4$ is considered, a critical point at each dash curve in Fig. 3 can be found to represent the critical traction for the given initial void size. A solid curve, Curve B, can be drawn by connecting the critical points, corresponding to the failure of the void surface material, of all dash curves for various initial void sizes. In other words, curve B represents the critical tractions for various initial void sizes.

When we examine the trend of curve B, we can identify that the critical traction for an initially small void is 2.0 MPa with consideration of the failure criterion. This critical traction represents the critical condition for an infinitesmal void when the rubber on the void surface fails at the large stretch ratio. This value is lower than 2.5 MPa predicted by the bifurcation model of cavitation. Also, curve B shows that as r_b/r_0 approaches to 1, the traction p_o becomes 0 at $R_b/r_0 = 4$. This can be explained by considering a spherical rubber shell with an infinitesmal thickness subject to radial expansion. The thin shell fails when the stretch ratio of the rubber reaches the critical value of 4 at $R_0/r_0 \approx R_b/r_0 = 4$.

For the Mooney-Rivlin material with the material constants given in Equations 14 to 16, the dead-load tractions (p_0) as functions of the normalized current void size (R_b/r_0) are shown as dash curves in Fig. 4 for various normalized initial void sizes (r_b/r_0). For the Mooney-Rivlin material, the critical traction is unbounded according to the bifurcation analysis in [22]. As shown in Fig. 4, when the normalized initial void size r_b/r_0 becomes small, the dash curves tend to the vertical line $R_b/r_0 = 0$. Therefore, an infinitesimal void cannot suddenly grow in the Mooney-Rivlin material when no failure criterion is considered. As for the neo-Hookean material, when the strain failure criterion at $\lambda = 4$ is considered, a solid curve can be drawn in Fig. 4 to represent the critical tractions for various normalized initial void sizes, where the stretch ratio λ

of the void surface material element meets the failure criterion at $\lambda = 4$. As the normalized initial void size becomes small, the solid curve approaches to a critical traction at 4.1 MPa.

For the JGS material characterized by the material constants in Equations 9 to 13, the dead-load tractions (p_0) as functions of the normalized current void size (R_b/r_0) are shown as dash curves in Fig. 5 for various normalized initial void sizes (r_b/r_0). For the JGS material, the critical traction should be unbounded according to the bifurcation analysis in [22]. As shown in Fig. 5, when the normalized initial void size r_b/r_0 becomes small, the dash curves tend to the vertical line $R_b/r_0 = 0$. Therefore, an infinitesimal void cannot suddenly grow in the JGS material when no failure criterion is considered. As for the neo-Hookean and Mooney-Rivlin materials, when the strain failure criterion at $\lambda = 4$ is considered, a solid curve can be drawn in Fig. 5 to represent the critical tractions for various normalized initial void sizes. As the normalized initial void size becomes small, the solid curve approaches to a critical traction near 3.0 MPa.

The dead-load tractions p_0 as functions of the normalized current void size R_b/r_0 are shown in Figs 3–5 for the NH, MR, and JGS materials, respectively. When we design for the maximum dead-load radial traction for a spherical thick shell with consideration of the failure criterion, the best design will be the cases with the normalized void size r_b/r_o from 0.4 to 0.7, where the dead-load radial tractions are maximized.

For a small void in the rubber particle, when the outer radius increases, the stretch ratio of the void surface element increases and meets the failure criterion. Then a thin layer of the surface element fails and loses the load-carrying capacity. As the radial displacement continues to increase, the stretch ratio of the next thin layer of rubber increases and fails. When the radial displacement further increases, more inner portion of the rubber particle fails and loses the load-carrying capacity. When all the rubber material elements are stretched and failed, the particle completely loses the load-carrying capacity and the radial traction becomes zero. This concept of gradual loss of load-carrying capacity of material elements or structures has been adopted in fracture mechanics and material modeling research, for example, see Jeong and Pan [14] on near-tip deformation pattern in rubber-modified epoxies and Tvergaard and Needleman [37] on ductile fracture in tensile bars. Of course, we assume a highly idealized deformation mode here because a spherically symmetrical model is needed to explore the post-bifurcation behavior of the rubber particle. We can simulate numerically the small void growth model as discussed above. However, there is another way to get the post-bifurcation behavior of the rubber particle with an infinitesmal void.

Fig. 6 shows the undeformed and deformed configurations of the rubber particle. In the figure, the rubber particle deformed radius R_o becomes sufficiently large so that the stretch ratio of the inner portion of the rubber particle is larger than the failure stretch ratio $\lambda = 4$. Denote the deformed radius of the material with the failure stretch ratio $\lambda = 4$ as R_f. The stretch ratio of the

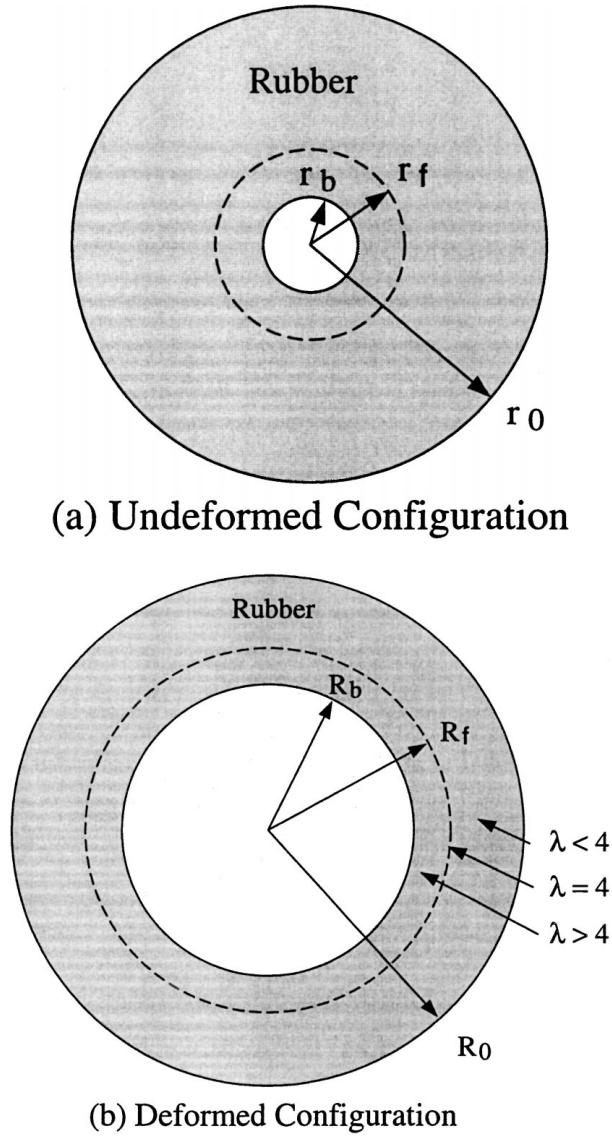

Figure 6 A void in a spherical rubber particle under radial traction. (a) undeformed configuration, (b) deformed configuration. In (b), the stretch ratio λ equal to the failure stretch ratio of 4 at the deformed radius R_f. The inner portion of the particle has the stretch ratio larger than 4 and has no load-carrying capacity. The outer portion of the particle has the stretch ratio less than 4 and carries the load. In (a), r_f represents the undeformed radius corresponding to R_f.

material with the current radius R less than R_f is larger than $\lambda = 4$. When the stretch ratio is larger or equal to 4, the rubber material fails. Therefore the inner portion of the particle has failed and has no load-carrying capacity. The load will then be carried by the outer portion of the particle. Consequently, the load-carrying capacity of the rubber particle at the current R_o can be obtained from the load-carrying capacity of the particle with the initial void radius r_f which is the undeformed radius corresponding to R_f.

Therefore, the dead-load traction of the rubber particle with an infinitesmal void should follow the curves for the critical tractions for various initial void sizes shown in Figs 3–5. In fact, Curve B in Fig. 3 and the solid curves in Figs 4 and 5 represent the plots of p_0's as functions of R_f/r_o for the rubber particle with an infinitesmal void. Based on the curves for the critical tractions and the incompressibility condition, the

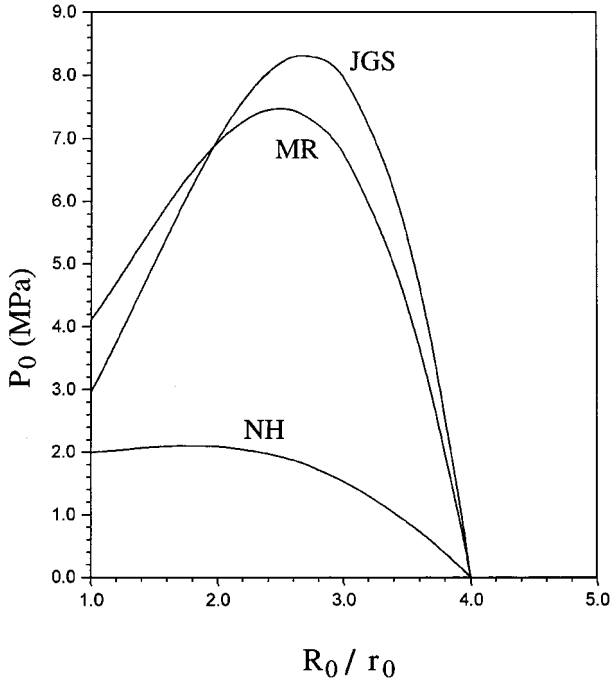

Figure 7 The dead-load tractions p_0 for the particle with an infinitesimal void are plotted as functions of the normalized particle size R_o/r_o for the neo-Hookean, MR and JGS materials with consideration of rubber failure at $\lambda = 4$.

dead-load tractions for an infinitesmal void are plotted as functions of the normalized particle size R_o/r_o for the NH, MR and JGS materials in Fig. 7. Note that the normalized deformed particle size R_o/r_o is used as the abscissa. It is easy to use the incompressibility condition to change the plot from p_0 as a function of R_o/r_o to p_0 as a function of R_b/r_o, as in most cavitation research works. However, we plot p_0 as a function of R_o/r_o because the inner portion of the particle fails and carries no load. Then it makes sense to plot p_0 as a function of R_o/r_o. Nevertheless, the plots as functions of R_o/r_o are quite similar to those as functions of R_b/r_o.

As shown in Fig. 7, these curves represent the post-bifurcation behaviors for the rubber particle containing an infinitesmal void with consideration of the failure criterion. Note that the dead-load tractions approach to finite values when R_o/r_o approaches to 1 (or R_b/r_o approaches to 0) as indicated by the numerical results. The dead-load tractions approach to zero as R_o/r_o approaches to the failure stretch ratio $\lambda = 4$. As shown in the the figure, there are maximum dead-load tractions for the three materials. Beyond these maximum dead-load tractions, no solution can be found according to this rate-independent, quasi-static approach.

The numerical results shown in Fig. 7 indicate the existence of cavitation stress for the three materials with consideration of the failure criterion. The existence of cavitation stress can be explained by the bifurcation approach of Horgan and Abeyaratne [21]. Horgan and Polignone [22] indicate that the existence of cavitation stress depends upon the behavior of the strain energy function at large stretch ratios. When the material is sufficiently soft at large stretch ratios, cavitation stress exists. When a failure criterion is assumed at finite stretch ratios, the material has zero load-carrying capacity and can be viewed as an extremely soft material at the stretch ratios larger than the failure stretch ratio. Therefore, for both lower-order and higher-order strain energy functions, cavitation stress exists when a failure criterion is assumed at a finite stretch ratio.

From the mathematical viewpoint, Equation 2.41 for cavitation stress p_{cr} in Horgan and Polignone [22] can be used to explain the numerical results shown in this paper. However, in order to make a direct use of the equation, the strain failure criterion should be modified slightly. In our strain failure criterion, the load-carrying capacity drops from a finite value to zero at the failure stretch ratio. However, in the modified strain failure criterion, the load-carrying capacity of the rubber increases to the maximum and then gradually decreases to zero near the failure stretch ratio so that the equation in Horgan and Polignone [22] can be integrated. This gradual loss of the load-carrying capacity is quite similar to that in the cohesive zone model extensively used in fracture mechanics (for example, see Kanninen and Popelar [38]). The cavitation stress according to the equation is obtained by integrating from 1 to infinity. With the failure criterion, the cavitation stress is obtained by integrating from 1 to a finite failure stretch ratio. Therefore, for the neo-Hookean material, the cavitation stress 2.0 MPa which is less than the value of 2.5 MPa without consideration of the failure criterion. When the failure stretch ratio increases to infinity, the cavitation stress without consideration of the failure criterion is recovered as indicated by the equation. For higher-order strain energy functions, the values of cavitation stresses will depend on failure stretch ratios and strain energy functions. For the MR and JGS materials, the cavitation stresses are at 4.1 and 3.0 MPa, respectively. Note that the biaxial stretching behaviors for the MR and JGS materials are much stiffer than that for the neo-Hookean material, as shown in Fig. 1. Therefore, the cavitation stresses for the MR and JGS materials are larger than that for the neo-Hookean material with the same failure stretch ratio. This can also be explained by the equation qualitatively.

In this paper, no physical dimension is given to the initial void size r_b. Surface energy becomes important as the physical dimension of the void becomes small. As shown in Gent and Wang [27], the critical stretch ratio depends upon the physical dimension of the void (or crack). However, their results show that when the void size decreases, the critical stretch ratio approaches to a constant. Here we have selected the critical stretch ratio as 4. Other values can be selected. Even we can select the critical stretch ratio as a function of the physical dimension of the void. But the qualitative results will be the same as those presented here.

5. Conclusions

In this paper, we investigate the spherical void expansion in spherical rubber particles under dead-load traction conditions. Spherical symmetry is assumed to simplify the governing equations in order to gain qualitative understanding of the cavitation phenomenon. We adopt a simple strain failure criterion for rubber at large strains. When a simple strain failure criterion is

employed, critical cavitation stresses of the order of the shear modulus exist consistently in nonlinearly elastic materials with different strain energy functions, in contrast to the results obtained without consideration of a failure mechanism.

Acknowledgement

The initial support of this work by the NSF under grant number DMR-8708405 is appreciated. Helpful discussions with Professors I. W. Chen and A. S. Wineman of the University of Michigan and Professor C. O. Horgan of the University of Virginia are appreciated.

References

1. A. F. YEE and R. A. PEARSON, *J. Mater. Sci.* **21** (1986) 2462.
2. R. A. PEARSON and A. F. YEE, *ibid.* **21** (1986) 2475.
3. *Idem., ibid.* **26** (1991) 3828.
4. A. F. YEE, D. LI and X. LI, *ibid.* **28** (1993) 6392.
5. H.-J. SUE and A. F. YEE, *Polymer Engineering and Science* **36** (1996) 2320.
6. A. LAZZERI and C. B. BUCKNALL, *J. Mater. Sci.* **28** (1993) 6799.
7. *Idem., Polymer* **36** (1995) 2895.
8. C. B. BUCKNALL and A. LAZZERI, *J. Mater. Sci.* **35** (2000) 427.
9. Y. HUANG and A. J. KINLOCH, *ibid.* **27** (1992) 2753.
10. A. C. STEENBRINK, E. VAN DER GIESSEN and P. D. WU, *Journal of the Mechanics and Physics of Solids* **45** (1997) 405.
11. A. C. STEENBRINK and E. VAN DER GIESSEN, *ibid.* **47** (1999) 843.
12. X.-H. CHEN and Y.-W. MAI, *J. Mater. Sci.* **34** (1999) 2139.
13. B. J. P. JANSEN, S. RASTOGI, H. E. H. MEIJER and P. J. LEMSTRA, *Macromolecules* **32** (1999) 6283.
14. H.-Y. JEONG and J. PAN, *Polymer Engineering and Science* **36** (1996) 2306.
15. W. J. CHANG and J. PAN, *International Journal of Fracture* **88** (1997) 61.
16. A. AL-ABDULJABBAR and J. PAN, *Polymer Engineering and Science* **39** (1999) 662.
17. A. N. GENT and P. B. LINDLEY, *Proceedings of the Royal Society of London* **A249** (1959) 195.
18. M. F. ASHBY, F. J. BLUNT and M. BANNISTER, *Acta Metallurgica* **37** (1989) 1847.
19. R. HILL, "The Mathematical Theory of Plasticity" (Clarendon Press, Oxford, 1950).
20. J. M. BALL, *Philosophical Transactions of the Royal Society of London* **A306** (1982) 557.
21. C. O. HORGAN and R. ABEYARATNE, *Journal of Elasticity* **16** (1986) 189.
22. C. O. HORGAN and D. A. POLIGNONE, *Applied Mechanics Reviews* **48** (1995) 471.
23. Y. HUANG, J. W. HUTCHINSON and V. TVERGAARD, *Journal of the Mechanics and Physics of Solids* **39** (1991) 223.
24. V. TVERGAARD, Y. HUANG and J. W. HUTCHINSON, *European Journal of Mechanics, A/Solids* **11** (1992) 215.
25. H. HOU and R. ABEYARATNE, *Journal of the Mechanics and Physics of Solids* **40** (1992) 571.
26. M. L. WILLIAMS and R. A. SCHAPERY, *International Journal of Fracture Mechanics* **1** (1965) 64.
27. A. N. GENT and C. WANG, *J. Mater. Sci.* **26** (1991) 339.
28. B. G. KAO and L. RAZGUNAS, On the determination of strain energy functions of rubbers. SAE paper number 860816, Society of Automotive Engineers, 1986.
29. A. G. JAMES, A. GREEN and G. M. SIMPSON, *J. Appl. Polym. Sci.* **19** (1975) 2033.
30. A. G. JAMES and A. GREEN, *ibid.* **19** (1975) 2319.
31. C. TRUESDELL and W. NOLL, in "Encyclopedia of Physics III/3," edited by S. Fluegge (Springer-Verlag, Berlin, 1965).
32. W. GOLDBERG, PhD thesis, Purdue University, 1967.
33. K. N. MORMAN, JR., B. G. KAO and J. C. NAGTEGAAL, Fourth International Conference on Vehicle Structural Mechanics, Detroit, Michigan, 1981, pp. 83–92.
34. J. T. ODEN, "Finite Elements of Nonlinear Continua" (McGraw-Hill, New York, 1972).
35. M.-S. CHOU-WANG and C. O. HORGAN, *International Journal of Solids and Structures* **25** (1989) 1239.
36. D. A. POLIGNONE and C. O. HORGAN, *Journal of Elasticity* **33** (1993) 27.
37. V. TVERGAARD and A. NEEDLEMAN, *Acta Metallurgica et Materialia* **32** (1984) 157.
38. M. F. KANNINEN and C. F. POPELAR, "Advanced Fracture Mechanics" (Oxford University Press, New York, 1985).

Received 31 March
and accepted 26 August 2000